ment of CBF at 2 and 24 h after administration of L-745,870 (210 mg/kg) or vehicle. Cerebral blood flow was measured by the hydrogen clearance method via a platinum wire electrode stereotaxically inserted into the right hippocampus using coordinates of 2 mm posterior and 2 mm lateral to the bregma, and 2.5 mm below the brain surface in a flat cranial presentation, as previously reported (Osuga *et al*, 2000).

Histopathology

After 3 days of reperfusion, animals were anesthetized with 4% halothane and perfused with 60 mL of 4% paraformaldehyde in phosphate buffer (pH 7.4) via a catheter placed in the heart. The brains were removed, fixed in 10% formalin for 10 days, and embedded in paraffin. Paraffin sections were sliced at a thickness of 7 μm for histopathologic and immunohistochemical evaluation. Neuronal cell density of the CA1 subfield of the hippocampus, that is, the number of intact CA1 pyramidal neurons per 1 mm linear length of pyramidal cell layer, was measured by counting 7 μm sections stained with hematoxylin and eosin from 3 to 7 independent animals in a double-masked manner.

Immunohistochemistry

Brain sections were subjected to NAIP and XIAP immunohistochemistry with polyclonal anti-human NAIP (ME1) and XIAP antibodies (R&D Systems Inc.), respectively, and stained using the Vectastain elite ABC kit (Vector Laboratories Inc., Burlingame, CA, USA) according to the manufacturer's instructions. In brief, after deparaffinization, the sections were washed with 0.01 mol/L PBS (pH 7.2) for 5 mins and were incubated with anti-NAIP (5 μg/mL) or anti-XIAP (5 μg/mL) antibody overnight at 4°C. The sections were rinsed three times with PBS containing 0.05% Triton X-100 for 10 mins, incubated with biotinylated secondary antibody for 3 h, and then incubated with avidin–biotin–peroxidase complex for 1 h at room temperature. Finally, the sections were treated with 0.5% 3,3′-diaminogenzidine (DAB) and 0.01% H_2O_2 in Tris-HCl buffer (pH 7.5), and the DAB reaction products were observed under a microscope.

Statistical Analysis

All data in this study are presented as mean ± s.e. Data were analyzed for significance using Student's *t*-test for pair-wised comparisons or ANOVA followed by Scheffe's test for multiple comparisons between groups (Statview 5.0 software; SAS, Cary, NC, USA). A *P*-value <0.05 was considered as reaching statistical significance.

Results

Identification of NAIP Upregulating Compounds

To identify compounds with the ability to induce NAIP expression, 953 compounds (Tocris) were screened using NAIP-ELISA. Compounds were arbitrarily categorized as 'downregulator' ($n=16$) if the resulting NAIP level was less than 70% of the normal endogenous level (i.e., ~12 ng/mL), or 'upregulator' ($n=30$) if the resulting NAIP level was more than 200% of the normal endogenous NAIP level (Table 1).

To examine whether the 30 identified NAIP upregulators suppressed menadione-induced cell death, THP-1 cell viability assays were performed in cells pretreated with menadione followed by the addition of each NAIP upregulator. All 30 compounds exerted a protective effect against menadione-induced cell death with variable degrees (Table 1). The compound that exerted the most potent protective effect was L-745,870, a dopamine D4 receptor antagonist (Figure 1A). This compound was used for subsequent experiments.

L-745,870 Protects a Variety of Cultured-Cells Against Menadione-Induced Cell Death

To determine whether the protective effect of L-745,870 on THP-1 cells was specific to cell type, cell viability studies were also conducted in HeLa and SH-SY5Y (differentiated neuroblastoma by all-*trans*-retinoic acid treatment) cells after exposure to the compound. L-745,870 protected both cell lines from menadione-induced cell death (Figures 1A, THP-1; B, HeLa; and C, SH-SY5Y). Further, the dose-

Table 1 Screening of 953 Tocris compounds by NAIP-ELISA, and viability assays after challenging with menadione-induced oxidative stress in THP-1 cells

NAIP level	*NAIP concentration*			*Cell viability (%)*
	Mean ± s.e. (ng/mL)	*Minimum (ng/mL)*	*Maximum (ng/mL)*	*(n) (menadione; 40 μmol/L)*
Untreated (control)	12.4 ± 0.3 (240)	11.8	12.7	31–37% (30)
Compound treated				
Unchanged	12.9 ± 0.4 (907)	10.1	21.3	ND*
Upregulator	54.8 ± 12.1 (30)	31.8	78.8	45–93% (30)
Downregulator	8.6 ± 0.8 (16)	7.1	9.1	ND*

NAIP, neuronal apoptosis inhibitory protein; ELISA, enzyme-linked immunosorbent assay; *ND, not determined. Number in each parenthesis indicates the number of tested compounds.

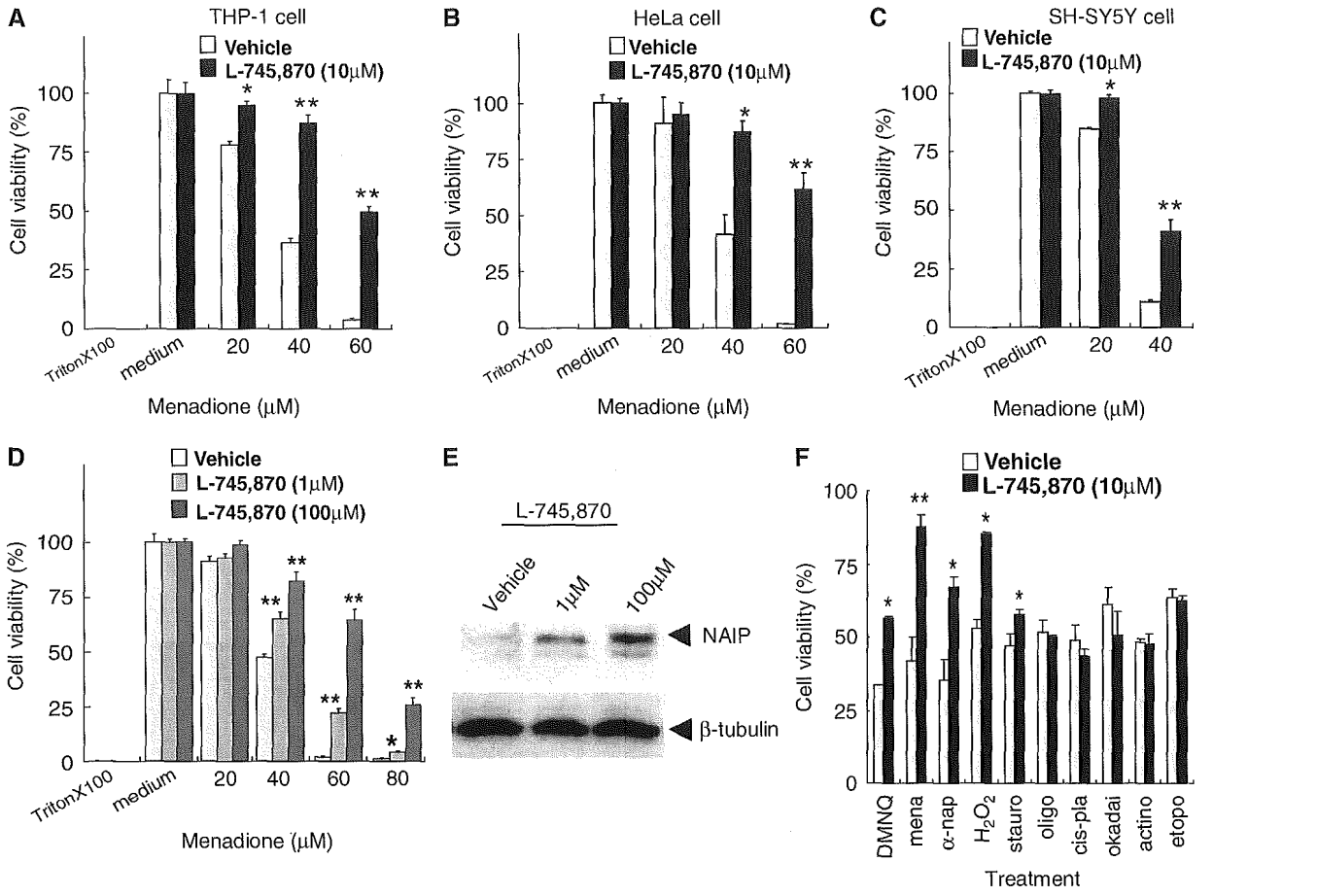

Figure 1 The effect of L-745,870 on oxidative stress-induced cell death. Cell viability after menadione treatment in (**A**) THP-1, (**B**) HeLa, and (**C**) differentiated SH-SY5Y cells was assayed. Cells that were pretreated with vehicle or L-745,870 (10 μmol/L) for 24 h were challenged with menadione (0 to 100 μmol/L) for 4 h. Each value represents the percentages of the cell viability relative to those of control (Triton X-100-treated cells) (means ± s.e.; $n = 8$). $^*P < 0.01$; $^{**}P < 0.001$, versus each corresponding vehicle. Statistical analysis was performed using Student's *t*-test. (**D** and **E**) Effect of various concentrations of L-745,870 on neuronal apoptosis inhibitory protein (NAIP) expression and cell viability after menadione treatment in HeLa cells. (**D**) Cells were pretreated with vehicle or L-745,870 (1 and 100 μmol/L) for 24 h and then challenged with menadione (0 to 100 μmol/L) for 4 h. $^*P < 0.01$; $^{**}P < 0.001$, versus each corresponding vehicle. Statistical analysis was performed using ANOVA with Scheffe's *post hoc* test. (**E**) Western blotting analysis of NAIP in HeLa cells treated with L-745,870 (1 and 100 μmol/L) or vehicle for 24 h. The arrowhead indicates the position of NAIP (150 kDa). Expression of β-tubulin was not affected by L-745,870 treatment and shows that equal amount of proteins loaded in each lane of the blot. (**F**) Effects of L-745,870 on cell viability after exposure to cell death-inducing agents in HeLa cells. Cells were pretreated with vehicle or L-745,870 (10 μmol/L) for 24 h and then exposed to various reagents, including DMNQ, menadione (mena), α-naphthoquinone (α-na), H_2O_2, staurosporine (stauro), oligomycin (oligo), *cis*-platinum (*cis*-pla), okadaic acid (okadaic), actinomycin D (actino), and etoposide (etopo). $^*P < 0.01$; $^{**}P < 0.001$, versus each corresponding vehicle. Statistical analysis was performed using Student's *t*-test.

dependent increase in cell viability correlated with a concomitant increase in NAIP level in HeLa cells (Figures 1D and 1E).

L-745,870 Selectively Protects Cells Against Oxidative Stress-Induced Apoptosis

To gain insight into the suppression of the cell death with L-745,870, HeLa cells pretreated with L-745,870 were challenged with various apoptosis-inducing stimuli and chemical cell-stressors. L-745,870 specifically suppressed cell death induced by oxidative stressors, including cell death in response to menadione, hydrogen peroxide (H_2O_2), DMNQ, and α-naphthoquinone, but did not protect against cell death induced by nonoxidative stressors (e.g., staurosporine, oligomycin, *cis*-platinum, okadaic acid, actinomycin D, and etoposide) (Figure 1F).

To confirm the antiapoptotic effect of L-745,870 against oxidative stress-induced cell death, flow cytometric analysis of cell treated with L-745,870 and menadione and double-stained with Annexin V-FITC and PI was performed. Half of the population of the menadione-treated cells that were not

exposed to L-745,870 were distributed in the LR quadrant (early stage of apoptosis) in an early phase of incubation (60 mins) but subsequently shifted to the UR quadrant (apoptosis/necrosis) during the late phase of incubation (4 h) (data not shown). These data suggest that cell death in response to menadione is the result of apoptosis rather than necrosis. L-745,870 treatment reduced the apoptotic cell population in the UR quadrant from 45% to 20% and increased the LL and LR quadrant populations from 32% to 59% and 15% to 19%, respectively (Figure 2A). L-745,870 treatment also reduced the apoptotic cell population in the UR quadrant from 78% to 53% and increased the normal cells in the LL quadrant from 6% to 28% in the cells exposed to H_2O_2 for 40 mins (Figure 2B). These results suggest that L-745,870 specifically protects cells from apoptosis induced by oxidative stress.

L-745,870 Specifically Upregulates NAIP

To examine whether L-745,870 specifically induces NAIP expression level among the antiapoptotic proteins, expression levels of the IAP family (XIAP, cIAP-1, cIAP-2, and survivin) and Bcl-2 family (Bcl-2 and Bcl-XL) proteins were assessed in HeLa and SH-SY5Y cells by Western blotting. L-745,870 specifically elevated the endogenous level of NAIP (Figure 3A) but had no effect on the levels of other antiapoptotic proteins (Figures 3B–3G). This observation was consistent with results obtained by the DNAChip analysis (8,300 genes, including all of the known antiapoptotic proteins with the exception of the *NAIP/BIRC1* gene: the Atlas Plastic Arrays analysis; Beckton Dickinson), in which no upregulation of the antiapoptosis relating genes was observed (data not shown). Slight decreases in the levels of XIAP and cIAP-1 were noted only in differentiated SH-SY5Y cells (Figures 3B and 3C), although the physiologic significance for this small effect may not be significant. These results indicate that L-745,870 selectively enhances endogenous NAIP levels.

L-745,870 Inhibits Oxidative Stress-Induced Apoptosis Via NAIP Upregulation

To investigate whether the elevation of the endogenous NAIP level by L-745,870 is responsible for the protection against oxidative stress-induced apoptosis, *NAIP* gene expression was suppressed using NAIP-RNAi. Transfection of HeLa cells with NAIP-U6 resulted in a marked decrease in endogenous NAIP levels (Figure 4A) and a concomitant increase in susceptibility to menadione (Figure 4B). Further, L-745,870-treated/NAIP-U6 transfected HeLa cells showed higher susceptibility to menadione than cells with NAIP-U6 treatment alone (Figure 4B). These results indicate that the increased

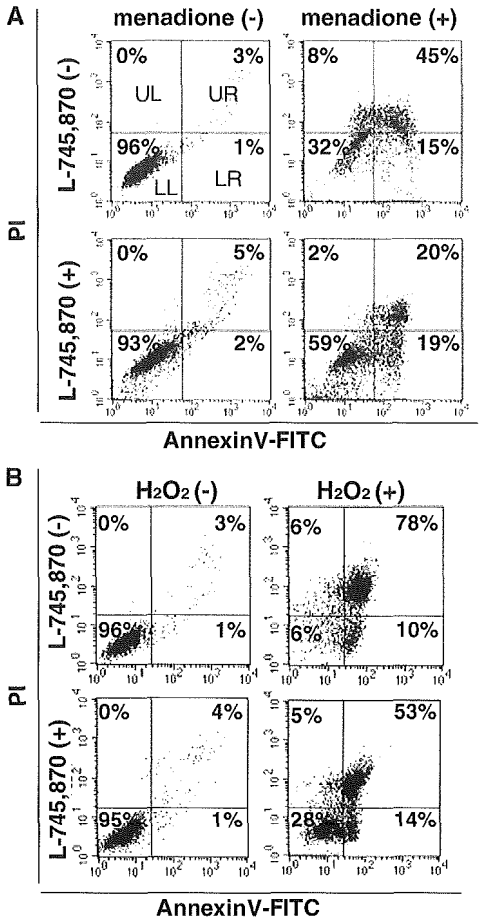

Figure 2 Effect of the neuronal apoptosis inhibitory protein (NAIP) upregulating compound (L-745,870) on the oxidative stress-induced apoptotic cell death, and a flow-cytometric analysis of the apoptotic and/or necrotic cell death in HeLa cells. HeLa cells that were precultured with vehicle or L-745,870 (10 μmol/L) for 24 h were challenged with (**A**) menadione (+: 50 μmol/L, for 4 h) or (**B**) H_2O_2 (+: 250 μmol/L, for 40 mins). Cell death was detected by staining with Annexin V-FITC and PI in conjunction with flow cytometry. FACS quadrant analysis allows the classification of the cells into four distinct categories based on the areas in the quadrant: upper left (UL), upper right (UR), low left (LL), and low right (LR). Percentage of the cell numbers in each quadrant is shown on the right.

endogenous NAIP level by L-745,870 likely mediates its ability to protect cells from oxidative stress-induced apoptosis.

Systemic Administration of L-745,870 Results in a Transient Upregulation of NAIP in Gerbil Hippocampal CA1 Neurons

L-745,870 administration had no effect on CBF (control/vehicle; 103.9±13.2 mL/100 g/min, 2 h after administration; 100.3±12.0 mL/100 g/min, and 24 h after administration; 98.9±13.2 mL/100 g/min;

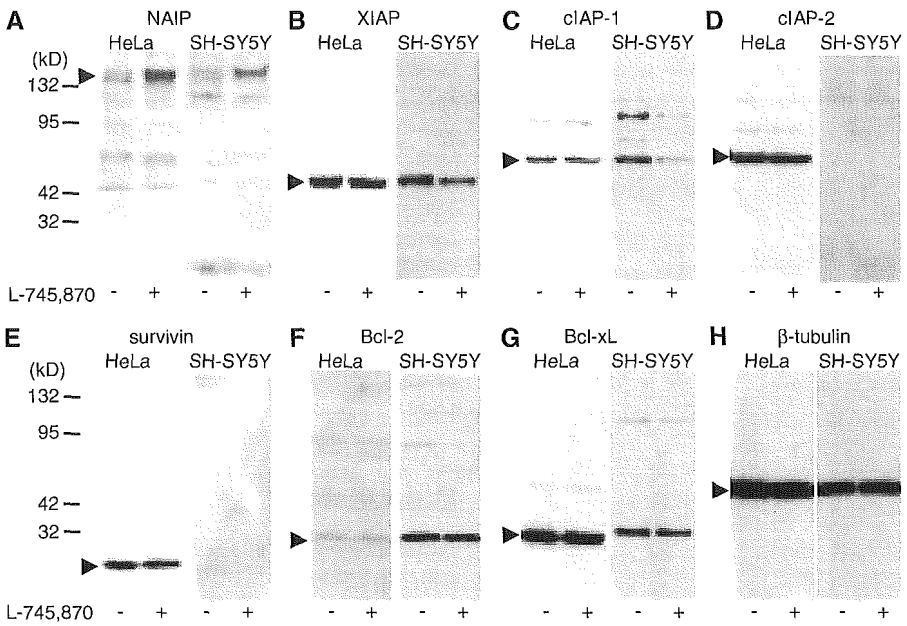

Figure 3 Western blot analysis of antiapoptotic proteins in HeLa and differentiated SH-SY5Y cells after treatment with L-745,870 (+, 10 μmol/L) or vehicle (−) for 24 h. Seven antiapoptotic proteins, including (**A**) neuronal apoptosis inhibitory protein (NAIP), (**B**) X-linked inhibitor of apoptosis (XIAP), (**C**) cIAP-1, (**D**) cIAP-2, (**E**) survivin, (**F**) Bcl-2, and (**G**) Bcl-xL, were analyzed. Each arrowhead indicates the position of each protein (NAIP: 150 kDa, XIAP: 47 kDa, cIAP-1: 65 kDa, cIAP-2: 64 kDa, survivin: 16.5 kDa, Bcl-2: 27 kDa, Bcl-xL: 28 kDa). (**H**) Expression of β-tubulin was not affected by L-745,870 treatment, showing that equal amounts of proteins were loaded in each lane of the blots.

control versus 2 h; $P>0.1$, control versus 24 h; $P>0.1$), blood pressure, and heart rate in gerbils (data not shown), which were consistent with results from a previous study (Patel *et al*, 1999). However, administration of L-745,870 (210 mg/kg) resulted in increased NAIP-immunoreactivity in the hippocampal CA1 neurons at 2 h (Figures 5A and 5B). Further, the increase in NAIP-immunoreactivity peaked at 24 h and then gradually returned to baseline at 72 h after administration (Figures 5A–5D). Results of the Western blotting were consistent with those obtained by the immunohistochemical studies (Figure 5E).

Administration of L-745,870 Attenuates Ischemia-Induced neuronal Cell Death in the Hippocampal CA1 Region

To determine whether administration of L-745,870 exerted neuroprotective against ischemic insults *in vivo*, gerbil forebrain ischemic models were established by transient BCCAO, which induces a selective loss of CA1 pyramidal cells in the hippocampus (Kirino and Sano, 1984). Because the time course of changes in NAIP expression occurred over a 72 h period after administration of L-745,870, the experimental protocol used induction of a relatively severe ischemic condition (10 min BCCAO), followed by the analysis of delayed neuronal loss in the CA1 region over the subsequent 72 h. At 72 h after the ischemic insult, vehicle treated animals showed widespread hippocampal CA1 neuron death with very few surviving neurons present in the pyramidal layer (Figures 6A and 6B). Further, a large number of glial cells were also observed in this area (Figures 6A and 6B). However, these animals showed little or no cell loss in the CA3 region or dentate gyrus (data not shown).

Administration of L-745,870 at 60 mins before the ischemic surgery exerted significant neuroprotective effects against ischemic insults in a concentration-dependent manner. A decreased dosage of L-745,870 (7 mg/kg) showed the most modest protection in the hippocampus CA1 neurons (data not shown), whereas medium to high dosages (70 and 210 mg/kg) exhibited prominent protective effects (Figures 6C–6F). The quantitative scoring of the neuronal cell damage was consistent with these results (Figure 6I). Moreover, the highest dose of L-745,870 (210 mg/kg) was not associated with any CA1 neuron toxicity (Figures 6G and 6H). Further, these protective effects were significant even at 5 days after reperfusion in this experimental condition, despite the fact that progressive cell death in CA1 neurons was observed (data not shown). Together, these results indicate that L-745,870 inhibits progression of the ischemia-induced CA1 neuron death.

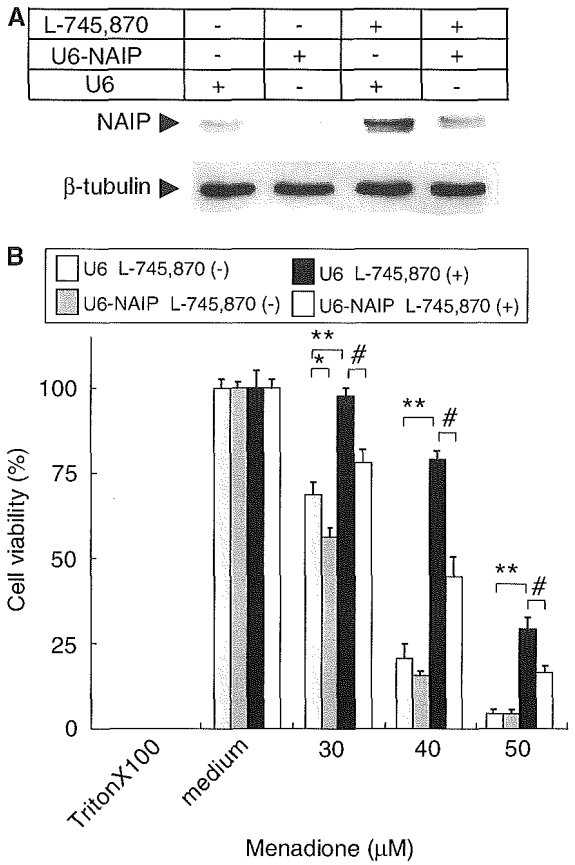

Figure 4 Effect of inhibition of neuronal apoptosis inhibitory protein (NAIP) expression on menadione-induced cell death in HeLa cells. Neuronal apoptosis inhibitory protein RNAi was achieved by ectopically expressing the small interference RNA (siRNA) corresponding to a portion of the 3′-UTR of the *NAIP* gene using the pSilencer 1.0-U6 system. (**A**) Western blot analysis of the NAIP expression in the RNAi treated HeLa cells. The lower panel represents the expression of β-tubulin and showed that equal amounts of protein were loaded in each lane in the blot. (**B**) Effect of the NAIP RNAi on menadione-induced cell death, and on the protection of cell death by L-745,870. Concentration of menadione used in this experiment was between 30 and 50 μmol/L. Cell viability is shown as percentages of the alamarBlue values in U6 or NAIP-U6-transfected cells relative to those of controls (menadione non-treated). Values represent the means ± s.e. of eight independent experiments. $^{*}P<0.01$ and $^{**}P<0.001$ for U6 L-745,870 (−) cells versus NAIP-U6 L-745,870 (+) cells or U6 L-745,870 (+). $^{\#}P<0.001$ for U6 L-745,870 (+) cells versus NAIP-U6 L-745,870 (+) cells. Statistical analysis was performed using Student's *t*-test.

Hippocampal CA1 Neurons Rescued by the Administration of L-745,870 Show Strong NAIP-Immunoreactivity

To investigate whether L-745,870-mediated hippocampal CA1 neuronal protection was associated with elevation of neuronal NAIP levels, immunohistochemical and Western blot analyses of endogenous NAIP were performed in CA1 neurons using an NAIP antibody. After 72 h of reperfusion, the CA1 neurons showed significant enhancement of the NAIP-immunoreactivity in the rescued neurons in a dose-dependent manner (Figures 7A–7F). Results of the Western blotting were consistent with results obtained by immunohistochemical studies (Figure 7H). In contrast, L-745,870 produced no detectable upregulation of XIAP-immunoreactivity in the rescued hippocampus (Figures 7G and 7H). These results show that L-745,870 selectively upregulates NAIP *in vivo*, which represent a potential mechanism by which L-745,870 exerts a neuroprotective effect against ischemia in hippocampal CA1 neurons.

Discussion

Neuronal apoptosis inhibitory protein (BIRC1) is the founding member of the IAP family of proteins, and has been shown to inhibit apoptosis of neurons and other types of the cell *in vitro* and *in vivo*. Increases in NAIP, by either viral-mediated NAIP gene transfer or by enhancement of endogenous levels, results in the attenuation of ischemic neuronal cell death (Xu *et al*, 1997). Further, ectopic NAIP expression enhances rescue of motor neurons from peripheral nerve axotomy (Perrelet *et al*, 2000) and leads to preservation of nigrostriatal dopaminergic neurons in the intrastriatal 6-OHDA rat Parkinson's disease model (Crocker *et al*, 2001). Neuronal apoptosis inhibitory protein also contributes to motor neuron survival through intracellular signaling of GDNF (Perrelet *et al*, 2002). Ischemic neuronal injury is associated with excessive generation of reactive oxygen species (ROS) and oxidative stress in the brain (Chan, 1994; Mattson *et al*, 2001; Friedlander, 2003), and the present study showed that NAIP suppresses neuronal cell death by exerting an antiapoptotic function against oxidative stress.

Most tissues and cells, with the exception of hematopoietic tissues, express NAIP in very low levels (Yamamoto *et al*, 1999). Thus, upregulation of endogenous NAIP in neuronal cells may represent a potent therapeutic strategy for prevention of neurodegeneration. Among the 30 NAIP upregulating compounds identified, two compounds, L-745,870 (dopamine D4 receptor antagonist) and bromocriptine (dopamine D2 receptor agonist; data not shown), exerted particularly prominent protection against neurodegeneration in an ischemia gerbil model. A previous study showed that bromocriptine protected neuronal cells from oxidative stress-induced apoptosis (Schapira, 2002), while another study showed that a number of other dopamine D2 receptor agonists attenuated neuronal cell death under ischemic conditions (Liu *et al*, 1995). L-745,870 was originally identified as a specific antagonist for the dopamine D4 receptor and as a drug candidate for antipsychotic treatment because

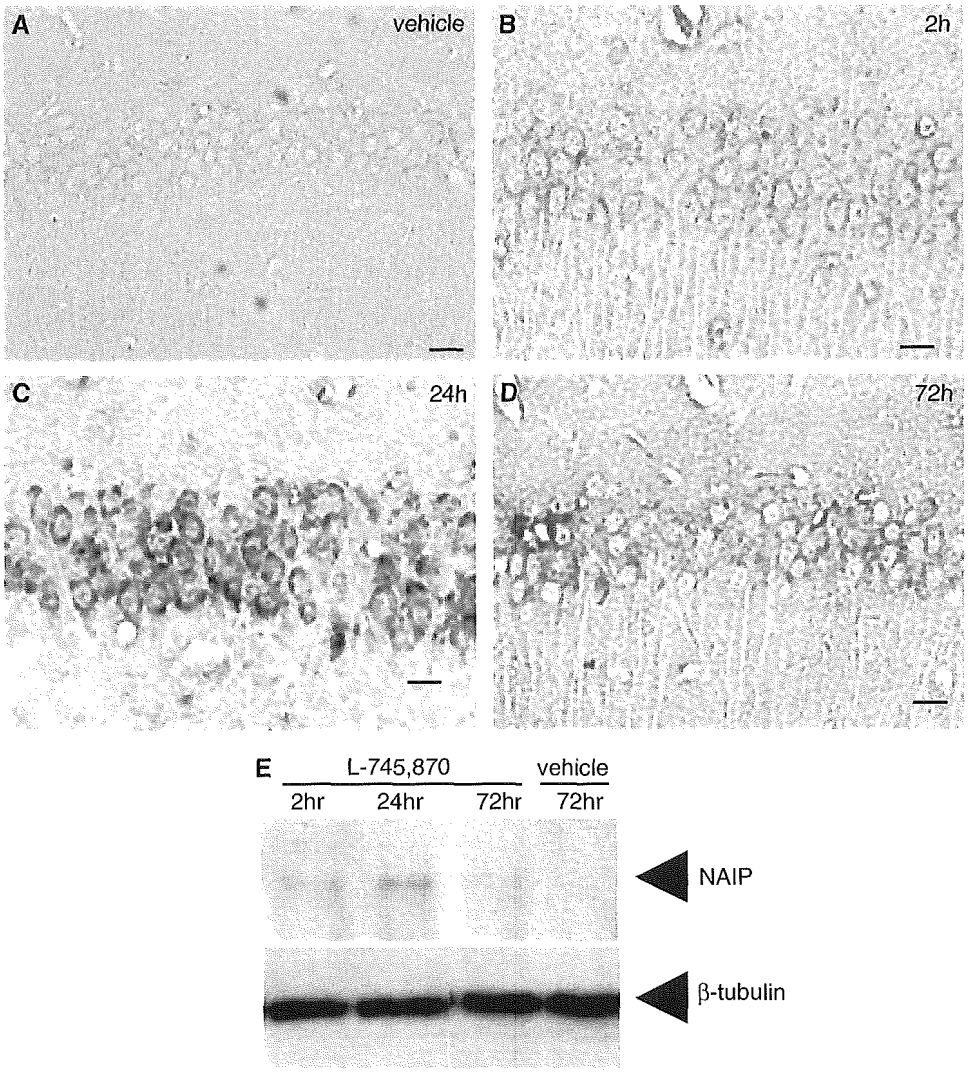

Figure 5 Upregulation of neuronal apoptosis inhibitory protein (NAIP) by L-745,870 in CA1 neurons. Adult gerbils were treated with vehicle (**A**) or L-745,870 (210 mg/kg; **B–D**). Representative coronal brain sections at the level of the dorsal hippocampus at 2, 24, and 72 h after administration of L-745,870 (210 mg/kg) are shown (**B–D**). Tissues were immunostained with the NAIP polyclonal antibody (ME1). Scale bar: 20 μm in higher magnification (× 400; **A–D**). (**E**) Western blot analysis of NAIP in hippocampus at 2, 24, and 72 h (L-745,870; 210 mg/kg) and 72 h (vehicle) after the administration of either L-745,870 or vehicle. Upper and lower panels represent the expression of NAIP and β-tubulin, respectively. Arrows indicate the proteins of interest (NAIP: 150 kDa). Expression of β-tubulin demonstrates equal loading in each lane.

of its excellent oral bioavailability and brain penetration (Patel *et al*, 1997). The present study showed the novel finding that L-745,870 specifically elevated the endogenous NAIP level and enhanced neuronal cell resistance to oxidative stress-induced apoptotic cell death and ischemic neurodegeneration.

The dopamine D4 receptor is a G-protein-coupled receptor that shares sequence homology with the D2 and D3 receptors and is classified as a member of the dopamine D2-like receptors group (Baldessarini, 1997). However, the action of L-745,870 in the present study is likely not mediated via dopaminergic receptors, because the antiapoptotic properties of L-745,870 against oxidative stress-induced cell death were observed in both differentiated dopaminergic SH-SY5Y cells, in which several types of dopamine receptors are expressed (Kamakura *et al*, 1997), and in nonneuronal cells, which do not express these receptors. Indeed, recent reports suggest that the dopamine agonists, bromocriptine and pergolide, act as free radical scavengers (Yoshikawa *et al*, 1994; Sam and Verbeke, 1995; Grünblatt *et al*, 1999) and exert their neuroprotective effects in nonreceptor-mediated fashions (Uberti *et al*, 2002). The present finding that L-745,870

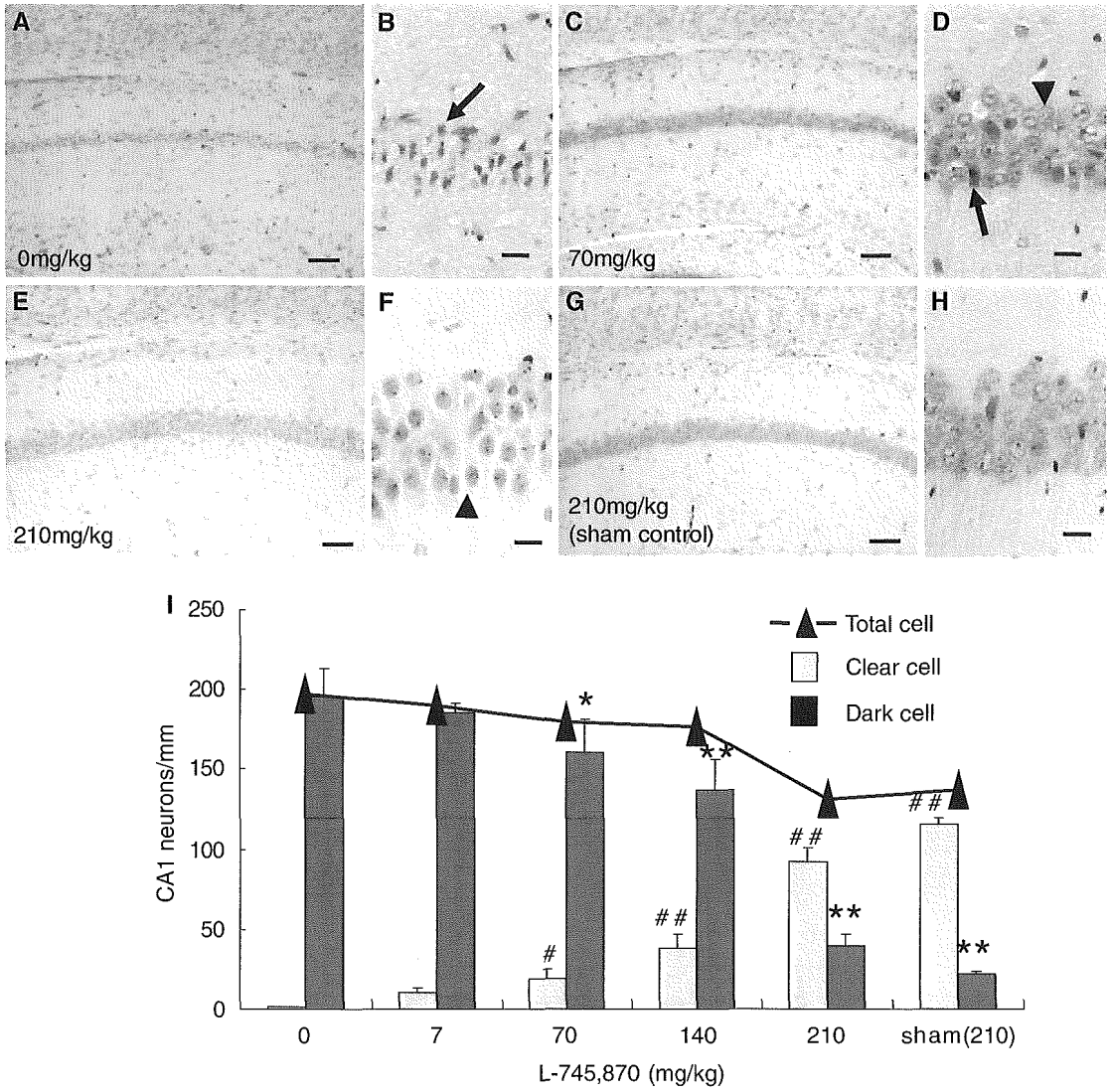

Figure 6 Effects of L-745,870 on ischemia-induced neuronal cell death in gerbils. Adult gerbils were treated with L-745,870 and then subjected to forebrain ischemia (bilateral common carotid artery occlusion (BCCAO) for 10 mins; **A–F**) or sham-operation (**G** and **H**). Representative coronal brain sections at the level of the dorsal hippocampus at 72 h (3 days) after reperfusion are shown. Tissues were stained with hematoxylin–eosin. Dosages of L-745,870 administered were 0 mg/kg (**A** and **B**), 70 mg/kg (**C** and **D**), and 210 mg/kg (**E–H**). Forebrain ischemia resulted in a significant loss of CA1 pyramidal cells. Scale bar: 100 μm in lower magnification ($\times$ 100; **A**, **C**, **E**, and **G**); 20 μm in higher magnification ($\times$ 400; **B**, **D**, **F**, and **H**). Arrowheads and arrows indicate dark (damaged) and clear (living) cells, respectively. (**I**) Number of pyramidal cells in the CA1 subfield of the hippocampus (cells/mm length of pyramidal cell layer). Both living (clear) and damaged (dark) CA1 neurons were count from six to seven animals in each experiment in a double-masked manner, and the values are represented as means $\pm$ s.e. Total numbers of CA1 pyramidal neurons (filled triangles; clear + dark cells) are also shown. $^{*}P<0.01$; $^{**}P<0.001$, compared with dark cells of vehicle-treated control (0 mg/kg). $^{\#}P<0.001$; $^{\#\#}P<0.001$, compared with clear cells of vehicle-treated control (0 mg/kg). Statistical analysis was performed using ANOVA with Scheffe's *post hoc* test.

may exert its neuroprotective via increases in NAIP, either by increasing its expression or stabilization, may provide a mechanism by which all of these effector molecules exert their effects.

The present study showed that L-745,870 upregulated NAIP but not other antiapoptotic proteins. Further, L-745,870 specifically protected both neuronal and nonneuronal cultured cells from apoptosis induced by several oxidative stressors, including DMNQ, menadione, α-naphthoquinone, and H_2O_2. This increase in NAIP likely mediates the protective effect of L-745,870 because reduction of NAIP expression with RNAi inhibited the neuroprotective effect. Recent studies have shown that NAIP suppresses caspase-dependent and -independent apoptosis (Deveraux *et al*, 1997, 1998; Roy *et al*,

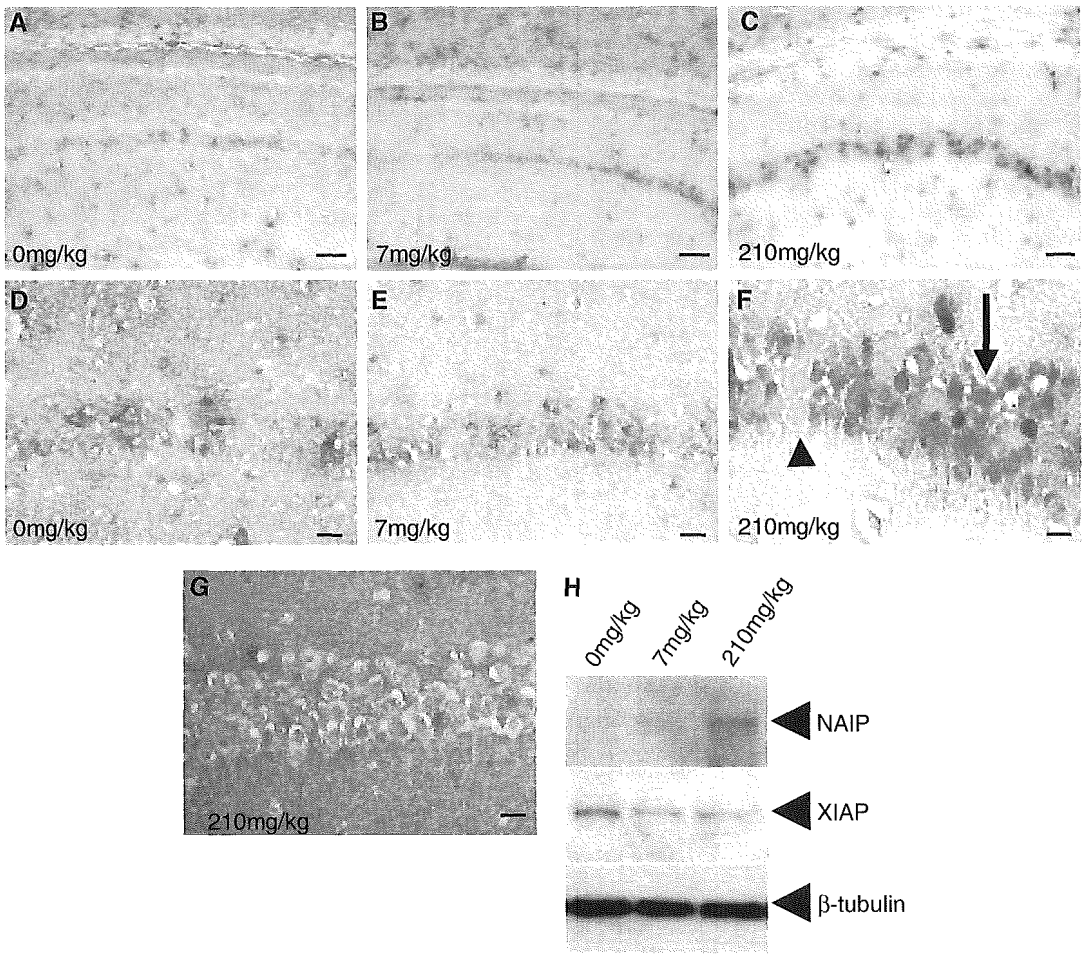

Figure 7 Effect of L-745,870 on expression of neuronal apoptosis inhibitory protein (NAIP) in CA1 neurons of ischemic gerbils. Adult gerbils were treated with L-745,870 and then subjected to forebrain ischemia (bilateral common carotid artery occlusion (BCCAO) for 10 mins; **A–G**). Representative coronal brain sections at the level of the dorsal hippocampus at 72 h (3 days) after reperfusion are shown (**A–G**). Tissues were immunostained with NAIP polyclonal antibody (ME1). Dosages of L-745,870 administered were 0 mg/kg (**A** and **D**), 7 mg/kg (**B** and **E**), and 210 mg/kg (**C**, **F**, and **G**). Scale bar: 100 μm in lower magnification ($\times$ 100; **A–C**); 20 μm in higher magnification ($\times$ 400; **D–G**). (**F**) Arrow and arrowhead indicate the NAIP-positive and negative cell, respectively. (**G**) Immunostaining of X-linked inhibitor of apoptosis (XIAP) in CA1 neurons of ischemic gerbil pretreated with L-745,870 (210 mg/kg). (**H**) Western blot analysis of NAIP and XIAP in hippocampus at 72 h (3 days) after ischemia. Upper, middle, and lower panels represent the expression of NAIP, XIAP, and β-tubulin, respectively. Each arrow indicates a position of the protein of interest (NAIP: 150 kDa, XIAP: 47 kDa). Expression of β-tubulin demonstrates equal loading in each lane.

1997; Seshagiri and Miller, 1997; Takahashi *et al*, 1998; Maier *et al*, 2002), while we previously showed that the antiapoptotic effect of NAIP was mediated by the caspase-3-independent pathway (Sakai *et al*, unpublished). Further studies to characterize the molecular mechanisms of NAIP upregulation and subsequent inhibition of oxidative stress-induced cell death would be of benefit.

It is notable that L-745,870 slightly but consistently downregulates the levels of both XIAP and cIAP-1 in differentiated SH-SY5Y cells. Recent studies have shown that a group of the ring finger-containing members of IAP family protein, such as XIAP and cIAP, can function as ubiquitin protein ligases, and regulates the levels of not only their target proteins but also themselves through ubiquitylation (Yang *et al*, 2000; Salvesen and Duckett, 2002). Thus, it is possible that L-745,870 may affect the stability of these IAP proteins via regulating the proteasome-dependent protein degradation. Equally likely is that this compound directly or indirectly modulates the expression of these genes and/or proteins in SH-SY5Y cells. Further studies will be needed to clarify the molecular mechanism underlying this inhibitory effect. Nevertheless, as the downregulation of XIAP and cIAP-1 is expected to exert the opposite effect to antiapoptosis, the decreases in XIAP and cIAP-1 observed in this study may not be a primary determinant for the antiapoptotic function associated with L-745,870.

We also showed that L-745,870 attenuated ischemia-induced CA1 neuronal cell death with concomitant increase in the NAIP expression in rescued CA1 neurons. Indeed, selective upregulation of NAIP might mediate a broad range of protection against oxidative stress-induced cell death. For example, a previous study has shown that the small molecule alkaloid, K252a, which is structurally quite different from L-745,870, upregulated NAIP levels and exerted a significant protective effect against ischemic damage in hippocampal CA1 neurons (Xu *et al*, 1997).

In conclusion, the dopamine D4 receptor antagonist, L-745,870, exerts a potent neuroprotective effect against ischemia-induced cell death via increases in NAIP. Since L-745,870 is clinically well tolerated (Bristow *et al*, 1997), this compound may represent an effective therapeutic strategy for the clinical prevention of neuronal cell death after ischemia. Future studies not only on the molecular mechanism by which L-745,870 induces the NAIP expression but also on the effectiveness of this compound in various ischemic conditions will clarify therapeutic potentials of L-745,870 in the treatment of several types of acute as well as chronic neurodegenerative diseases caused by oxidative stress. Further, our NAIP-ELISA-based drug screening may facilitate the discovery of novel neuroprotective compounds.

Acknowledgements

The authors thank Dr Kenji Yamamoto and all the members of our laboratory for their scholarly input.

References

Baldessarini RJ (1997) Dopamine receptors and clinical medicine. In: *The dopamine receptors* (Neve KA, Neve RL, eds), Totowa, NJ: Humana, 457–98

Bristow LJ, Kramer MS, Kulagowski J, Patel S, Ragan CI, Seabrook GR (1997) Schizophrenia and L-745,870, a novel dopamine D4 receptor antagonist. *Trends Pharmacol Sci* 18:186–8

Chan PH (1994) Oxygen radicals in focal cerebral ischemia. *Brain Pathol* 4:59–65

Crocker SJ, Wigle N, Liston P, Thompson CS, Lee CJ, Xu D, Roy S, Nicholson DW, Park DS, MacKenzie A, Korneluk RG, Robertson GS (2001) NAIP protects the nigrostriatal dopamine pathway in an intrastriatal 6-OHDA rat model of Parkinson's disease. *Eur J Neurosci* 14: 391–400

Crowther JR (1995) *ELISA: theory and practice.* Totowa, NJ: Humana

Deveraux QL, Takahashi R, Salvesen GS, Reed JC (1997) X-linked IAP is a direct inhibitor of cell-death proteases. *Nature* 388:300–4

Deveraux QL, Roy N, Stennicke HR, Van Arsdale T, Zhou Q, Srinivasula SM, Alnemri ES, Salvesen GS, Reed JC (1998) IAPs block apoptotic events induced by caspase-8 and cytochrome *c* by direct inhibition of distinct caspases. *EMBO J* 17:2215–23

Friedlander RM (2003) Apoptosis and caspases in neurodegenerative diseases. *N Engl J Med* 348:1365–75

Gavrilov DK, Shi X, Das K, Gilliam TC, Wang CH (1998) Differential SMN2 expression associated with SMA severity. *Nat Genet* 20:230–41

Graham SH, Chen J (2001) Programmed cell death in cerebral ischemia. *J Cereb Blood Flow Metab* 21:99–109

Grünblatt E, Mandel S, Gassen M, Youdim MBH (1999) Potent neuroprotective and antioxidant activity of apomorphine in MPTP and 6-hydroxydopamine induced neurotoxicity. *J Neural Transm Suppl* 55:57–70

Hsieh-Li HM, Chang JG, Jong YJ, Wu MH, Wang NM, Tsai CH, Li HA (2000) Mouse model for spinal muscular atrophy. *Nat Genet* 24:66–70

Kamakura S, Iwaki A, Matsumoto M, Fukumaki Y (1997) Cloning and characterization of the 5′-flanking region of the human dopamine D4 receptor gene. *Biochem Biophys Res Commun* 235:321–6

Kirino T, Sano K (1984) Fine structural nature of delayed neuronal death following ischemia in the gerbil hippocampus. *Acta Neuropathol (Berlin)* 62:209–18

Krajewski S, Mai JK, Krajewska M, Sikorska M, Mossakowski MJ, Reed JC (1995) Upregulation of bax protein levels in neurons following cerebral ischemia. *J Neurosci* 15:6364–76

Liu XH, Kato H, Chen T, Kato K, Itoyama Y (1995) Bromocriptine protects against delayed neuronal death of hippocampal neurons following cerebral ischemia in the gerbil. *J Neurol Sci* 129:9–14

Love S (1999) Oxidative stress in neurological disease. *Brain Pathol* 9:119–31

Maier JK, Lahoua Z, Gendron NH, Fetni R, Johnston A, Davoodi J, Rasper D, Roy S, Slack RS, Nicholson DW, MacKenzie AE (2002) The neuronal apoptosis inhibitory protein is a direct inhibitor of caspases 3 and 7. *J Neurosci* 22:2035–43

Mattson MP, Duan W, Pedersen WA, Culmsee C (2001) Neurodegenerative disorders and ischemic brain diseases. *Apoptosis* 6:69–81

Monani UR, Sendtner M, Coovert DD, Parsons DW, Andreassi C, Le TT, Jablonka S, Schrank B, Rossol W, Prior TW, Morris GE, Burghes AH (2000) The human centromeric survival motor neuron gene (SMN2) rescues embryonic lethality in Smn(−/−) mice and results in a mouse with spinal muscular atrophy. *Hum Mol Genet* 9:333–9

Nitatori T, Sato N, Waguri S, Karasawa Y, Araki H, Shibanai K, Kominami E, Uchiyama Y (1995) Delayed neuronal death in the CA1 pyramidal cell layer of the gerbil hippocampus following transient ischemia is apoptosis. *J Neurosci* 15:1001–11

Osuga H, Osuga S, Wang F, Fetni R, Hogan MJ, Slack RS, Hakim AM, Ikeda JE, Park DS (2000) Cyclin-dependent kinases as a therapeutic target for stroke. *Proc Natl Acad Sci USA* 97:10254–9

Patel S, Freedman S, Chapman KL, Emms F, Fletcher AE, Knowles M, Marwood R, McAllister G, Myers J, Curtis N, Kulagowski JJ, Leeson PD, Ridgill M, Graham M, Matheson S, Rathbone D, Watt AP, Bristow LJ, Rupniak NM, Baskin E, Lynch JJ, Ragan CI (1997) Biological profile of L-745,870, a selective antagonist with high affinity for the dopamine D4 receptor. *J Pharmacol Exp Ther* 283:636–47

Perrelet D, Ferri A, MacKenzie AE, Smith GM, Korneluk RG, Liston P, Sagot Y, Terrado J, Monnier D, Kato AC

(2000) IAP family proteins delay motoneuron cell death *in vivo*. *Eur J Neurosci* 12:2059–67

Perrelet D, Ferri A, Liston P, Muzzin P, Korneluk RG, Kato AC (2002) IAPs are essential for GDNF-mediated neuroprotective effects in injured motor neurons *in vivo*. *Nat Cell Biol* 4:175–9

Raghupathi R, Graham DI, McIntosh TK (2000) Apoptosis after traumatic brain injury. *J Neurotrauma* 17:927–38

Roy N, Mahadevan MS, McLean M, Shutler G, Yaraghi Z, Farahani R, Baird S, Besner-Johnston A, Lefebvre C, Kang X, Salih M, Aubry H, Tamai K, Guan X, Loannou P, Crawford TO, Jong PJ, Ikeda JE, Korneluk RG, Mackenzie A (1995) The gene for neuronal apoptosis inhibitory protein is partially deleted in individuals with spinal muscular atrophy. *Cell* 80:167–78

Roy N, Deveraux QL, Takahashi R, Salvesen GS, Reed JC (1997) The c-IAP-1 and c-IAP-2 proteins are direct inhibitors of specific caspases. *EMBO J* 16:6914–25

Salvesen GS, Duckett CS (2002) IAP proteins: blocking the road to death's door. *Nat Rev Mol Cell Biol* 3:401–10

Sam EE, Verbeke N (1995) Free radical scavenging properties of apomorphine enantiomers and dopamine: possible implication in their mechanism of action in Parkinsonism. *J Neural Transm Park Dis Dement Sect* 10:115–27

Schapira AH (2002) Neuroprotection and dopamine agonists. *Neurology* 58:9–18

Seshagiri S, Miller LK (1997) Baculovirus inhibitors of apoptosis (IAPs) block activation of Sf-caspase-1. *Proc Natl Acad Sci USA* 94:13606–11

Takahashi R, Deveraux Q, Tamm I, Welsh K, Assa-Munt N, Salvesen GS, Reed JC (1998) A single BIR domain of XIAP sufficient for inhibiting caspases. *J Biol Chem* 273:7787–90

Uberti D, Piccioni L, Colzi A, Bravi D, Canonico PL, Memo M (2002) Pergolide protects SH-SY5Y cells against neurodegeneration induced by H(2)O(2). *Eur J Pharmacol* 434:17–20

Xu DG, Crocker SJ, Doucet JP, St-Jean M, Tamai K, Hakim AM, Ikeda JE, Liston P, Thompson CS, Korneluk RG, MacKenzie A, Robertson GS (1997) Elevation of neuronal expression of NAIP reduces ischemic damage in the rat hippocampus. *Nat Med* 3:997–1004

Xu DG, Bureau Y, McIntyre DC, Nicholson DW, Liston P, Zhu Y, Fong WG, Crocker SJ, Korneluk RG, Robertson GS (1999) Attenuation of ischemia-induced cellular and behavioral deficits by X chromosome-linked inhibitor of apoptosis protein overexpression in the rat hippocampus. *J Neurosci* 15:5026–33

Yamamoto K, Sakai H, Hadano S, Gondo Y, Ikeda JE (1999) Identification of two distinct transcripts for the neuronal apoptosis inhibitory protein gene. *Biochem Biophys Res Commun* 264:998–1006

Yang Y, Fang S, Jensen JP, Weissman AM, Ashwell JD (2000) Ubiquitin protein ligase activity of IAPs and their degradation in proteasomes in response to apoptotic stimuli. *Science* 288:874–7

Yoshikawa T, Minamiyama Y, Naito Y, Kondo M (1994) Antioxidant properties of bromocriptine, a dopamine agonist. *J Neurochem* 62:1034–8

予防医学事典

松島綱治
酒井敏行
石川　昌
稲寺秀邦
……[編集]……

朝倉書店

110　筋萎縮性側索硬化症原因遺伝子

筋萎縮性側索硬化症（amyotrophic lateral sclerosis：ALS）は，1次および2次運動ニューロンの選択的変性を特徴とする進行性神経性疾患である．欧米におけるALSの罹病率は人口10万人につき1～3とされており，わが国においても同等の高い発症頻度を示す疾患である．1869年にCharcotがALSの疾患概念を確立して以来130年以上が経過しているが，いまだALSの分子発症機構は明確ではなく，その治療法も確立されていない．ALS患者の大多数は孤発例であるが，5～10%の患者は家族性ALSと考えられている．近年の飛躍的な分子遺伝学の進歩により，家族性ALS遺伝子座が次々と明らかにされている．現在，優性遺伝形式をとる8種類のALS，および劣性遺伝形式をとる2種類のALSの遺伝子座が決定されている（表）．さらに，ALS関連遺伝子としてneurofilamentあるいはvascular endothelial growth factor（VEGF）などの遺伝子異常がALS発症・進行に関与していることも明らかにされつつある（表）．以下に，これまでに同定された代表的なALS原因・関連遺伝子について概説する．詳細に関しては，原著（表中：文献）ならびに総説[1~5]を参照していただきたい．

1.　*SOD1*：優性遺伝形式を示すALS1原因遺伝子

1993年，Rosenらは常染色体優性遺伝形式を示す家族性ALS1型の原因遺伝子Cu/Zn superoxide dismutase（*SOD1*）を発見した．*SOD1*遺伝子は，わずか154アミノ酸残基からなる小さい蛋白質をコードする遺伝子であるが，すでに100以上の遺伝子変異が報告されている（http://alsod1.iop.kcl.ac.uk/）．現在では，ALS1型はSOD1本来の機能の喪失によりもたらされるのではなく，変異蛋白質が細胞に対する毒性を獲得する，いわゆる「gain-of-toxic-function」により引き起こされるものと考えられている．このgain-of-toxic-functionの実体に関しては，異常リン酸化仮説，異常蛋白質蓄積説，さらにそれに伴う軸索輸送障害，細胞内小器官移送異常などの仮説が有力視されている．

2.　*ALS2*：劣性遺伝形式を示すALS2原因遺伝子

2001年，筆者らは常染色体劣性遺伝形式をとる若年発症型ALS2型の原因遺伝子（*ALS2*）を同定した．さらに最近，*ALS2*遺伝子が，ALS2型に加えて家族性若年発症型原発性側索硬化症（primary lateral sclerosis, juvenile：PLSJ）および小児発症上向性痙性麻痺（infantile-onset ascending hereditary spastic paralysis：IAHSP）の原因遺伝子であることも判明した[4]．ALS2蛋白質は，Rab5低分子量G蛋白質の活性化の触媒因子であり，細胞内ではその作用を介してエンドソーム動態調節・物質移送にかかわっていると想定されている[6]．したがって，ALS2/PLSJ/IAHSP患者においては，*ALS2*遺伝子変異によって生じる細胞内物質移送系の異常が運動ニューロンの機能障害・細胞死を引き起こしているものと考えられる．

3.　ALS関連遺伝子群

ALSの発症あるいは進行との関連が明らかにされている遺伝子は，これまで多数同定されている（表）．なかでも，*VEGF*遺伝子プロモーター領域の遺伝子多型および血中低VEGFがALS発症と強く関連し，VEGFがALSのリスクファクターであることが明らかにされたことは特記すべき知見である．また最近では，Dynein/Dynactinなどの細胞内物質移送系分子群の異常と運動ニューロン疾患との関連も注目されている．

ALSの発症原因は1つではなく，数多くの遺伝的要因が関与していると考えられる．したがって，ALS発症の分子メカニズムを解明するには，今後もさらに未同定の家族性ALSの原因遺伝子ならびに孤発性ALSの原因および環境因子をも含めた関連因子を突き止めてゆくことが重要であろう．近年のALSを含めた運動ニューロン疾患研究の進歩は著しい．以下に掲げたWebサイトは常時情報の更新を行っており，最新の運動ニューロン疾患研究に関する知見を得ることができる（NEUROMUSCULAR DISEASE CENTER, Washington University；http://www.neuro.wustl.edu/neuromuscular/index.html, Online Mendelian Inheritance in Man（OMIM）；http://www.ncbi.nlm.nih.gov/entrez/query.fcgi?db=OMIM）．

参考文献

1）Julien J-P：Amyotrophic lateral sclerosis：Unfolding the toxicity of the misfolded. *Cell* **104**：581-591, 2001.

表 筋萎縮性側索硬化症（ALS）原因・関連遺伝子

類　型	遺伝形式	遺伝子	遺伝子座	発症期	OMIM	文　献
家族性 ALS						
ALS1	優性	*SOD1*	21q22.1	成人	#105400 /*147450	Rosen, et al: *Nature* **362**: 59, 1993
ALS2(juvenile type3)	劣性	*ALS2*	2q33	若年	#205100 /*606352	Hadano, et al: *Nature Genet* **29**: 166, 2001
PLSJ*	劣性	*ALS2*	2q33	若年	#606353	Yang, et al: *Nature Genet* **29**: 160, 2001
IAHSP*	劣性	*ALS2*	2q33	若年	#607225	Eymard-Pierre, et al: *Am J Hum Genet* **71**: 518, 2002
ALS3	優性	?	18q21	成人	*606640	Hand, et al: *Am J Hum Genet* **70**: 251, 2002
ALS4	優性	*SETX*	9q34	若年	*602433	Chen, et al: *Am J Hum Genet* **74**: 1128, 2004
SPG19*	優性	?	9q34	若年	*607152	
distal HMN*	優性	?	9q34	若年		Jonghe, et al: *Brain* **125**: 1320, 2002
ALS5(juvenile type1)	劣性	?	15q15-q22	若年	*602099	Hentati, et al: *Neurogenetics* **2**: 55, 1998
ALS6	優性	?	16q12.1-q12.2	成人	*608030	Abalkhail, et al: *Am J Hum Genet* **73**: 383, 2003
ALS7	優性	?	20p	成人	*608031	Sapp, et al: *Am J Hum Genet* **73**: 397, 2003
ALS8	優性	*VAPB*	20p13.3	成人	*608627	Nishimura, et al: *Am J Hum Genet* **75**: 822, 2004
ALSX	X 連鎖	?	Xp11-q12	成人		Siddique, et al: *Am J Hum Genet* **63**: A308, 1998
ALS-FTD*	優性	?	9q21-q22	成人	*105550	Hosler, et al: *JAMA* **284**: 1664, 2000
ALS-FTDP/DDPAC*	優性	*MAPT*	17q21	成人	#600274 /*157140	Wilhelmsen, et al: *Am J Hum Genet* **55**: 1159, 1994
juvenile type2	劣性	?	?	若年		Ben Hamida, et al: *Brain* **113**: 347, 1990
ALS 関連遺伝子（抜粋）						
neurofilament heavy chain		*NEFH*	22q12.1-q13.1		*162230	Figlewicz, et al: *Hum Mol Genet* **3**: 1757, 1994
vascular endothelial growth factor		*VEGF*	6p12		*192240	Lambrechts, et al: *Nature Genet* **34**: 383, 2003
peripherin		*PRPH*	12q12-q13		*170710	Corbo, Hays: *J Neuropathol Exp Neurol* **51**: 531, 1992
glutamate transporter (EAAT2)		*SLC1A2*	11p13-p12		*600300	Rothstein, et al: *Ann Neurol* **38**: 73, 1995
apolipoprotein E		*APOE*	19q13.2		*107741	Mui, et al: *Ann Neurol* **38**: 460, 1995
ciliary neurotrophic factor		*CNTF*	11q12.2		*118945	Orrel, et al: *J Neuorol Sci* **132**: 126, 1995
glutamate receptor (AMPA)		*GRIA1*	5p33		*138248	Carriedo, et al: *J Neurosci* **16**: 4069, 1996
apurinic apyrimidinic endonuclease		*APEX*	14q12		*107748	Olkowski, et al: *Neuroreport* **9**: 239, 1998

*PLSJ: juvenile primary lateral sclerosis, IAHSP: infantile ascending hereditary spastic paralysis, SPG: spastic paraplegia, distal HMN: distal hereditary motor neuropathy, FTD: front-temporal dementia, FTDP: frontotemporal dementia and parkinsonism complex, DDPAC: disinhibition-dementia-Parkinsonism-amyotrophy complex

2) Cleveland DW, Rothstein JD : From Charcot to Lou Gehrig : Deciphering selective motor neuron death in ALS. *Nature Rev Neurosci* **2** : 806-819, 2001.
3) Majoor-Krakauer D, Willems PJ, Hofmn A : Genetic epidemiology of amyotrophic lateral sclerosis. *Clin Genet* **63** : 83-101, 2003.
4) 秦野伸二：新しい家族性筋萎縮性側索硬化症遺伝子：*ALS2* －運動ニューロン疾患における分子接点－．医学のあゆみ **205** : 119-123, 2003.
5) Kunst CB : Complex genetics of amyotrophic lateral sclerosis. *Am J Hum Genet* **75** : 933-947, 2004.
6) Otomo A, et al : ALS2, a novel guani : nucleotide exchange factor for the small GTPase Rab5, is implicated in endosomal dynamics. *Hum Mol Genet* **12** : 1671-1687, 2003.

秦野伸二@東海大学

Mutant Androgen Receptor Accumulation in Spinal and Bulbar Muscular Atrophy Scrotal Skin: A Pathogenic Marker

Haruhiko Banno, MD, Hiroaki Adachi, MD, Masahisa Katsuno, MD, Keisuke Suzuki, MD, Naoki Atsuta, MD, Hirohisa Watanabe, MD, Fumiaki Tanaka, MD, Manabu Doyu, MD, and Gen Sobue, MD

Objective: **Spinal and bulbar muscular atrophy (SBMA) is a hereditary motor neuron disease caused by the expansion of a polyglutamine tract in the androgen receptor (AR). The nuclear accumulation of mutant AR is central to the pathogenesis of SBMA. Androgen deprivation with leuprorelin inhibits mutant AR accumulation, resulting in rescue of neuronal dysfunction in a mouse model of SBMA. This study aimed to investigate whether mutant AR accumulation in the scrotal skin is an appropriate biomarker of SBMA.** ***Methods:*** **Immunohistochemistry of both scrotal skin and the spinal cord was performed on five autopsied SBMA cases. Neurological severity and scrotal skin findings were studied in another 13 patients. Five other patients received subcutaneous injections of leuprorelin and underwent scrotal skin biopsy.** ***Results:*** **The degree of mutant AR accumulation in scrotal skin epithelial cells tended to be correlated with that in the spinal motor neurons in autopsy specimens, and it was well correlated with CAG repeat length and inversely correlated with the amyotrophic lateral sclerosis functional scale. Leuprorelin treatment inhibited mutant AR protein accumulation in the scrotal skin of SBMA patients.** ***Interpretation:*** **These observations suggest that scrotal skin biopsy findings are a potent pathogenic marker of SBMA and can be a surrogate end point in therapeutic trials.**

Ann Neurol 2006;59:520–526

Spinal and bulbar muscular atrophy (SBMA), also known as Kennedy's disease, is an adult-onset motor neuron disease characterized by muscle atrophy, weakness, contraction fasciculations, and bulbar involvement.[1–4] SBMA exclusively affects men in their 30s or 40s, and disease progression is slow.[1,5] The molecular basis of SBMA is the expansion of a trinucleotide CAG repeat, which encodes a polyglutamine (polyQ) tract, in the androgen receptor (AR) gene.[6] The CAG repeat numbers range from 38 to 62 in SBMA patients, whereas healthy individuals have 10 to 36 CAGs.[6,7] The number of CAGs is correlated with disease severity and is inversely correlated with age of onset,[8,9] as observed in other polyQ-related neurodegenerative diseases including Huntington's disease and several forms of spinocerebellar ataxia.[10]

Histopathologically, lower motor neurons are markedly depleted in the spinal cord and brainstem, and nuclear inclusions (NIs) containing the mutant and truncated AR with expanded polyQ are present in the residual motor neurons, as well as in cells of the scrotal skin and other visceral organs.[3,11,12] Although NIs are a disease-specific pathological marker, they may reflect a cellular protective response against the toxicity of abnormal polyQ-containing protein.[13] In contrast, the therapeutic effect of testosterone deprivation in our SBMA transgenic mouse model suggested that diffuse nuclear accumulation of mutant AR is a cardinal pathogenic process underlying neurological manifestations.[14,15] This hypothesis has also been clearly illustrated by the observation that the extent of diffuse nuclear accumulation of mutant AR, but not NIs, in the motor neurons of the spinal cord was closely related to CAG repeat length in autopsied SBMA cases.[16] Nuclear localization of the mutant protein has now been considered essential for inducing neuronal cell dysfunction and degeneration in the majority of polyQ diseases.[10]

A characteristic clinical feature of SBMA is that the disease occurs in male but not female individuals, even when they are homozygous for the mutation.[17,18] Several studies have clarified that the sex dependency of disease manifestation in SBMA arises from testosterone-dependent nuclear accumulation of mu-

From the Department of Neurology, Nagoya University Graduate School of Medicine, Showa-ku, Nagoya, Japan.

Received Sep 1, 2005, and in revised form Oct 4. Accepted for publication Oct 6, 2005.

Published online Dec 15, 2005 in Wiley InterScience (www.interscience.wiley.com). DOI: 10.1002/ana.20735

Address correspondence to Dr Sobue, Department of Neurology, Nagoya University Graduate School of Medicine, 65 Tsurumai-cho, Showa-ku, Nagoya 466-8550, Japan.
E-mail: sobueg@med.nagoya-u.ac.jp

tant AR.[14,15,19,20] Leuprorelin, a leuteinizing hormone–releasing hormone agonist that reduces testosterone release from the testis and inhibits nuclear accumulation of mutant AR, rescued motor dysfunction in male transgenic mice carrying the full-length human AR with expanded polyQ.[15]

Although data from transgenic mice studies indicated that androgen deprivation from leuprorelin treatment is a potent therapeutic agent for SBMA,[14,15] clinical experience using this drug for SBMA patients is limited.[21] Because long-term clinical trials are needed to establish the efficacy of therapeutics ameliorating disease progression in slowly progressive neurodegenerative diseases such as SBMA, an appropriate biomarker reflecting pathogenic processes of the disease is necessary. The aim of this study was to test the hypothesis that peripheral accumulation of mutant AR in the scrotal skin represents a suitable biomarker of SBMA that can be applicable as a surrogate end point in therapeutic trials.

Patients and Methods

Patients

Twenty-three patients with clinically and genetically confirmed SBMA were examined. Patient characteristics are shown in the Table. Five of the 23 patients underwent autopsy, and both the scrotal skin and the spinal cord were examined; another 13 patients underwent biopsy of the scrotal skin. The remaining five patients were enrolled in a leuprorelin study and also underwent biopsy of the scrotal skin. All patients were hospitalized and underwent follow-up examinations at Nagoya University Hospital (Nagoya, Japan) and its affiliated hospitals.

For each of the 18 patients who underwent biopsy of the scrotal skin, three scrotal skin specimens were made by punch biopsy using a 3mm diameter Dermapunch (Nipro, Tokyo, Japan) under 10ml lidocaine acetate local anesthesia. All patients who underwent biopsy sterilized the wound for several days by themselves and received 4 days of cefaclor (250mg three times a day) antibiotic therapy after the procedure. The 13 patients who underwent biopsy who were not enrolled in the leuprorelin trial were also assessed on the amyotrophic lateral sclerosis functional scale (limb Norris score), as described previously.[22]

Five other male subjects (age, 60–74 years; mean, 67.3 years) who died of nonneurological diseases served as control subjects. The Nagoya University Hospital Institutional Review Board approved the collection of data and specimens, and all patients gave their written, informed consent to participate.

Leuprorelin Administration

Five patients received subcutaneous injections of 3.75mg leuprorelin once every 4 weeks. The patients, aged 43 to 68 years, were capable of walking with or without a cane and expressed no desire to father a child. They were observed for 6 months (24 weeks), and scrotal skin biopsies were taken from each patient at 0, 4, and 12 weeks after initial leuprorelin administration. Serum creatine kinase (CK) was determined by ultraviolet measurement using hexokinase and glucose-6-phosphate. Serum testosterone levels were measured by radioimmunoassay using the DPC total testosterone kit (Diagnostic Products Corporation, Los Angeles, CA).

Immunohistochemical Detection of the Mutant Androgen Receptor in the Scrotal Skin and Spinal Cord

Immunohistochemistry of scrotal skin specimens and the spinal cord were conducted as described previously.[16] In brief, we prepared 5μm-thick, formalin-fixed, paraffin-embedded sections of scrotal skin and spinal cord from SBMA patients. Sections were deparaffinized and rehydrated through a graded series of alcohol-water solutions. For the mutant AR immunohistochemical study, sections were pretreated with immersion in 98% formic acid for 5 minutes, and then with microwave oven heating for 15 minutes in 10mM citrate buffer at pH 6.0. Sections were incubated with a mouse anti-expanded polyQ antibody (1:20,000; 1C2; Chemicon, Temecula, CA)[23] to evaluate the nuclear accumulation of mutant AR.[14–16] Immune complexes were visualized using the Envision-plus kit (Dako, Glostrup, Denmark). Sections were counterstained with Mayer's hematoxylin. For electron microscopic immunohistochemistry, the sections were processed

Table. Patient Characteristics

Characteristics	Autopsy Study (N = 5)	Biopsy Alone Study (N = 13)	Leuprorelin + Biopsy Study (N = 5)
Age (mean ± SD), yr	64.8 ± 10.8	54.8 ± 9.6	50.2 ± 10.8
Duration of weakness (mean ± SD), yr	38.4 ± 14.7	11.0 ± 7.4	8.8 ± 4.9
(CAG)n (mean ± SD)	47.4 ± 4.9	48.2 ± 3.0	49.2 ± 4.9
ADL (cane/independent ratio)	NA	4/9	2/3
Limb Norris score (mean ± SD)	NA	53.4 ± 6.9	52.0 ± 6.8
Norris bulbar score (mean ± SD)	NA	32.2 ± 3.4	32.8 ± 6.2
ALSFRS-R (Japanese edition) (mean ± SD)	NA	40.3 ± 3.2	39.2 ± 3.8
Cause of death	Pneumonia (n = 4); Lung cancer (n = 1)	NA	NA

The amyotrophic lateral sclerosis functional rating scale-revised.
SD = standard deviation; (CAG)n = number of expanded CAG repeats in the SBMA allele; NA = not applicable; ADL = activities of daily living.

as described for light microscopic immunohistochemistry, and then fixed with 2% osmium tetroxide in 0.1M phosphate buffer at pH 7.4, dehydrated in graded alcohol-water solutions, and embedded in epoxy resin. Ultrathin sections were cut for observation under an electron microscope (H-7100; Hitachi High-Technologies Corporation, Tokyo, Japan).

Quantification of Cell Population with Diffuse Nuclear Staining

For quantitative assessment of scrotal skin cells, the frequency of diffuse nuclear staining was calculated from counts of more than 500 nuclei in 5 randomly selected fields of each section photographed at 400× magnification (BX51TF; Olympus, Tokyo, Japan). To assess the nuclear accumulation of mutant AR in spinal cord motor neurons, we prepared at least 100 transverse sections each from the cervical, thoracic, and lumber spinal cord for anti-expanded polyQ antibody staining with 1C2. The numbers of 1C2-positive cells in the ventral horn on both the right and left sides were counted on every 10th section under the light microscope with a computer-assisted image analyzer (BX51TF; Olympus), as described previously.[16,24] Populations of 1C2-positive cells were expressed as percentages of the total skin cell or neuronal count.

Statistical Analysis

We analyzed the data by Pearson's coefficient, Spearman's rank correlation, and Student's paired t test as appropriate using StatView software (version 5; Hulinks, Tokyo, Japan) and considering p values less than 0.05 to be indicative of significance.

Results

Mutant Androgen Receptor Nuclear Accumulation in the Scrotal Skin and Spinal Motor Neuron

In the five autopsied cases, mutant AR nuclear accumulations were clearly visualized with anti-expanded polyQ immunostaining with 1C2 in the scrotal skin and spinal cord specimens (Fig 1A). Pathological accumulation of mutant AR was distributed in all layers of the epithelium. Diffuse nuclear accumulations were predominantly observed, and the occurrence of NIs was less frequent. This was also the case in the spinal cord specimens. Electron microscopic immunohistochemistry with the 1C2 antibody demonstrated granular dense and amorphous aggregates corresponding to diffuse nuclear staining in both spinal motor neurons and epithelial cells of scrotal skin (see Figs 1B, C). Filamentous structures such as those reported in Huntington's disease,[25] dentatorubal-pallidoluysian atrophy (DRPLA),[26] and Machado–Joseph disease[27] were not seen. No diffuse nuclear staining was seen in the control subjects. The extent of mutant AR accumulation in the scrotal skin epithelial cells showed a tendency to correlate with that in the anterior horn cells ($r = 0.84$; $p = 0.08$; see Fig 1D). Mutant AR accumulation was remarkable in both the spinal motor neurons and the scrotal skin of Patient 1, but was far less remarkable in Patient 2 (see Figs 1A, D).

Correlations of the Mutant Androgen Receptor Accumulation in the Scrotal Skin to CAG Repeat Length and Amyotrophic Lateral Sclerosis Score

Mutant AR nuclear accumulations in scrotal skin biopsies from the 13 SBMA patients who did not receive leuprorelin were assessed by 1C2 antibody staining of expanded PolyQ. The 1C2-positive cell population in the scrotal skin biopsies was significantly correlated with CAG repeat length ($r = 0.61$; $p = 0.03$; Fig 2A) and was inversely correlated with the functional scale assessed by the Norris score on limbs ($r = -0.63$; $p = 0.02$; see Fig 2B).

Leuprorelin Treatment Depletes Mutant Androgen Receptor Accumulation in the Scrotal Skin

In all five patients in which leuprorelin was administered (see the Table), both the intensity and the frequency of diffuse nuclear 1C2 staining in the scrotal epithelial cells was decreased after the first 4 weeks of administration compared with the preadministration values, and this effect was markedly enhanced after 12 weeks of treatment (Figs 3A, B). Quantitative analysis demonstrated a significant decrease in the frequency of 1C2-positive cells both 4 and 12 weeks after the initiation of leuprorelin treatment ($p < 0.01$) (see Fig 3C). Serum testosterone levels decreased to the castration level after 1 to 2 months of treatment (see Fig 3D), and serum CK values were also significantly decreased in all patients (see Fig 3D).

None of the patients showed the hot flush or obesity often reported in leuprorelin trials for prostate cancer. Although a loss of sexual function including erectile disorder was observed in all patients, no patients experienced depression. No marked exacerbations were observed in total cholesterol, triglyceride, fasting blood sugar, or HbA1c (data not shown). We could not find significant motor function changes assessed by amyotrophic lateral sclerosis functional scores in 24 weeks, but three of the five enrolled patients expressed apparent subjective improvement.

Discussion

This study demonstrated that scrotal skin biopsy with anti-expanded polyQ staining is a strong candidate for an appropriate biomarker with which to monitor SBMA pathogenic processes. Previous studies showed that the severity and progression of motor dysfunction and abatement of abnormalities in mice that were castrated or given leuprorelin paralleled the extent of diffuse nuclear mutant AR accumulation in their spinal motor neurons.[14,15] Furthermore, we demonstrated previously a significant, close correlation between the length of CAG repeat expansion and frequency of dif-

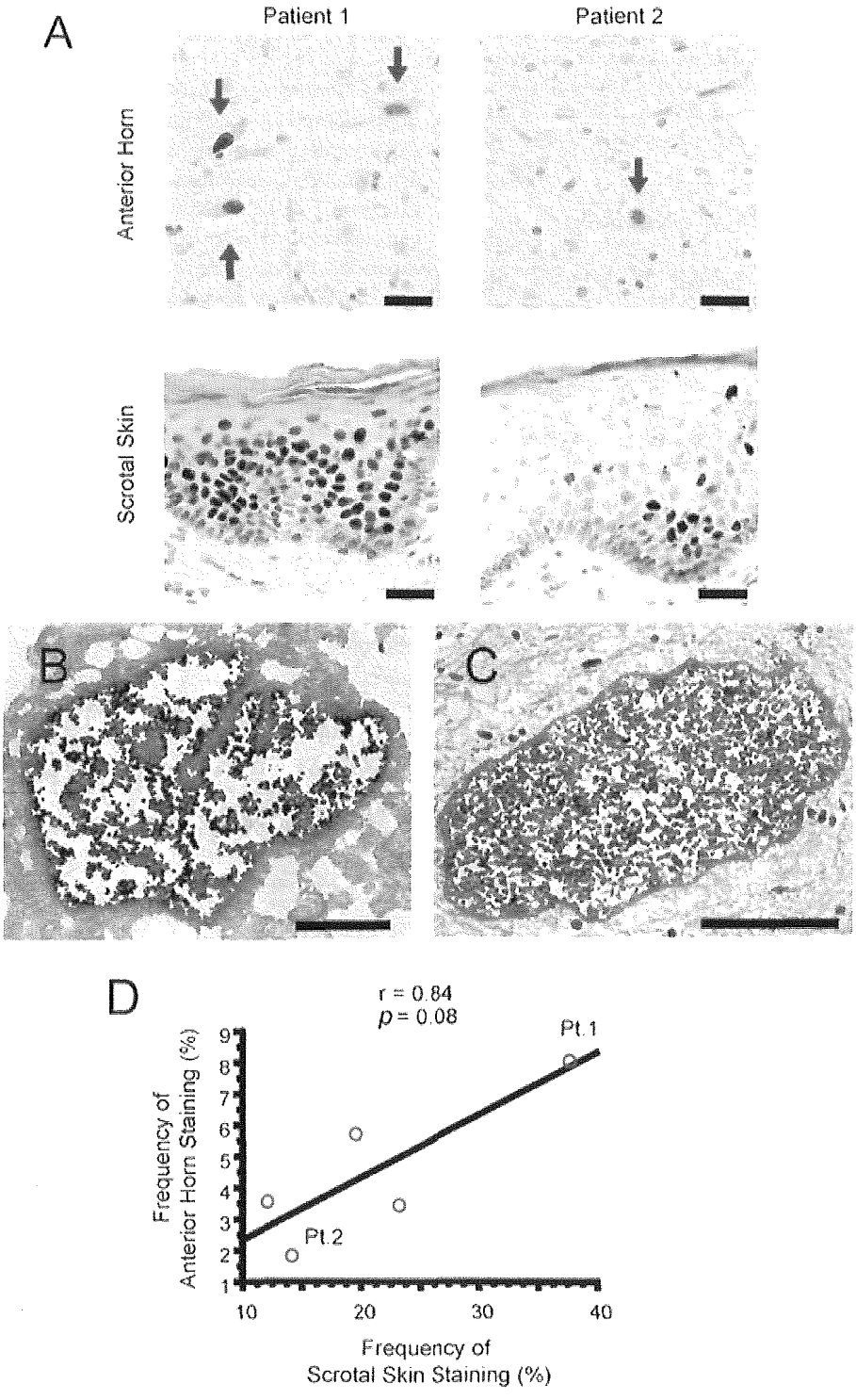

Fig 1. Mutant androgen receptor (AR) nuclear accumulation in scrotal skin and spinal motor neurons. (A) Mutant AR accumulation was remarkable in both spinal motor neurons (arrows) and scrotal skin of Patient 1, but was less remarkable in both motor neurons (arrows) and skin in Patient 2. Bar = 30μm. (B, C) Electron microscopic immunohistochemistry for 1C2 demonstrated granular dense and amorphous aggregates corresponding to diffuse nuclear staining in both spinal motor neurons and epithelial cells of scrotal skin. Bar =3μm. (D) The extent of mutant AR accumulation in scrotal skin epithelial cells showed a tendency to correlate with that in anterior horn cells. Circles (Pt. 1, Pt. 2) correspond to Patient 1 and 2 in Fig 1A.

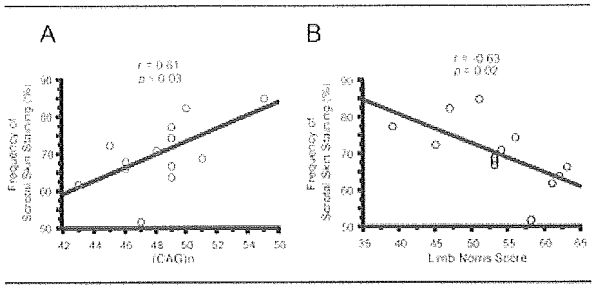

Fig 2. Correlation of the frequency of scrotal skin staining to CAG repeats and limb Norris score. The frequency of 1C2-positive cells in the scrotal skin biopsies correlated significantly with (A) CAG repeat length and (B) inversely correlated with the amyotrophic lateral sclerosis functional scale assessed by the Norris score on limbs. (CAG)n = number of expanded CAG repeats in the spinal and bulbar muscular atrophy allele.

fuse nuclear mutant AR accumulation, but not that of NIs, in the spinal cord.[16] Accordingly, neuronal dysfunction is likely to be caused by diffuse nuclear accumulation of mutant AR in the affected tissues. In this study, the extent of mutant AR nuclear accumulation in scrotal skin cells paralleled that in the anterior horn cells in autopsied cases. Electron microscopic immunohistochemistry for 1C2 anti-expanded PolyQ demonstrated granular dense and amorphous aggregates corresponding to diffuse nuclear staining in both spinal motor neurons and epithelial cells of scrotal skin. Furthermore, the fine structure of the aggregates in spinal motor neurons and epithelial cells was quite similar. Biopsy analyses in this study also suggested that scrotal skin findings were correlated with the motor functional scores of SBMA patients.

Our findings suggest that nuclear mutant AR assessed by 1C2 immunostaining in the scrotal skin is a practical procedure to estimate the severity of SBMA pathogenesis in the nervous system. In support of this view, decreases in mutant AR accumulation in the motor neurons paralleled that in nonneuronal cells in the androgen deprivation therapy tested in the mouse model of SBMA. In addition, leuprorelin treatment markedly reduced serum testosterone levels, as well as nuclear accumulation of mutant AR in the scrotal skin, suggesting that medical castration with leuprorelin intervenes in the pathogenic process of human SBMA, as demonstrated in the animal study. Moreover, serum CK levels were significantly decreased in this leuprorelin study. Because high CK values are common in SBMA patients and histopathological examinations have shown myogenic changes together with neurogenic findings in this disease,[1,3] presumably, a decrease in CK values with leuprorelin treatment implies muscular protection. Serum CK levels, however, did not significantly correlate with the Norris score on limbs or with scrotal skin biopsy findings in our cross-sectional study.

As defined by the Biomarkers Definitions Working Group, a disease biomarker should be objectively measurable and evaluated as an indicator of pathogenic processes or pharmacological responses to a therapeutic intervention.[28] Based on the observations described earlier, 1C2-stained mutant AR accumulation in the biopsied scrotal skin is likely to be a potent biomarker reflecting pathogenic processes of SBMA. Particularly, the correlation of the extent of mutant AR nuclear accumulation in the spinal motor neurons with that in scrotal skin biopsies in the autopsied cases suggests that findings in the scrotal skin can predict pathogenic processes in the motor neurons.

Although its precise natural history has not been evaluated, SBMA is a slowly progressive disease.[1,5] Thus, extremely long-term clinical trials are necessary to assess whether certain drugs can alter the natural disease progression by targeting clinical end points such as occurrence of aspiration pneumonia or becoming wheelchair bound. Suitable surrogate end points, which reflect the pathogenesis and severity of SBMA, are substantial to assess the therapeutic efficacy in drug trials. Although it is not practical to obtain biopsy specimens from the central nervous system (CNS), a punch biopsy of the scrotal skin enables a safe and accessible examination for patients.

It has also been suggested that reliance on surrogate end points can be misleading because they may not accurately predict the actual effects that treatments have on the health of a patient, as was seen with the CD4 counts in human immunodeficiency virus trials, the bone mineral density in osteoporosis trials, and others.[29] However, several factors have been suggested to consider the decision to rely on a surrogate.[30] In SBMA, mutant AR accumulation assessed by scrotal skin biopsy can be a candidate for a surrogate end point in light of several pieces of evidence. First, a credible SBMA animal model demonstrated dramatic functional motor recovery in response to testosterone deprivation therapy that depleted mutant AR accumulation in the central nervous system, as well as in nonneuronal tissues.[14,15] Second, the degree of diffuse nuclear accumulation of mutant AR in both the CNS and scrotal skin correlates well with CAG repeat length and disease severity, indicating that it is a natural phenomenon of and reflects the underlying pathology of the disease. Third, autopsy studies show that levels of nuclear AR accumulation in the scrotal skin are correlated with those in the CNS. Moreover, levels of nuclear translocated mutant AR in the scrotal skin decreased significantly in response to drug therapy that has been shown to deplete such accumulations in the CNS of SBMA mice, to significantly rescue motor dysfunction in these mice, and to partially stabilize neurological symptoms in one reported case of human SBMA.[21]

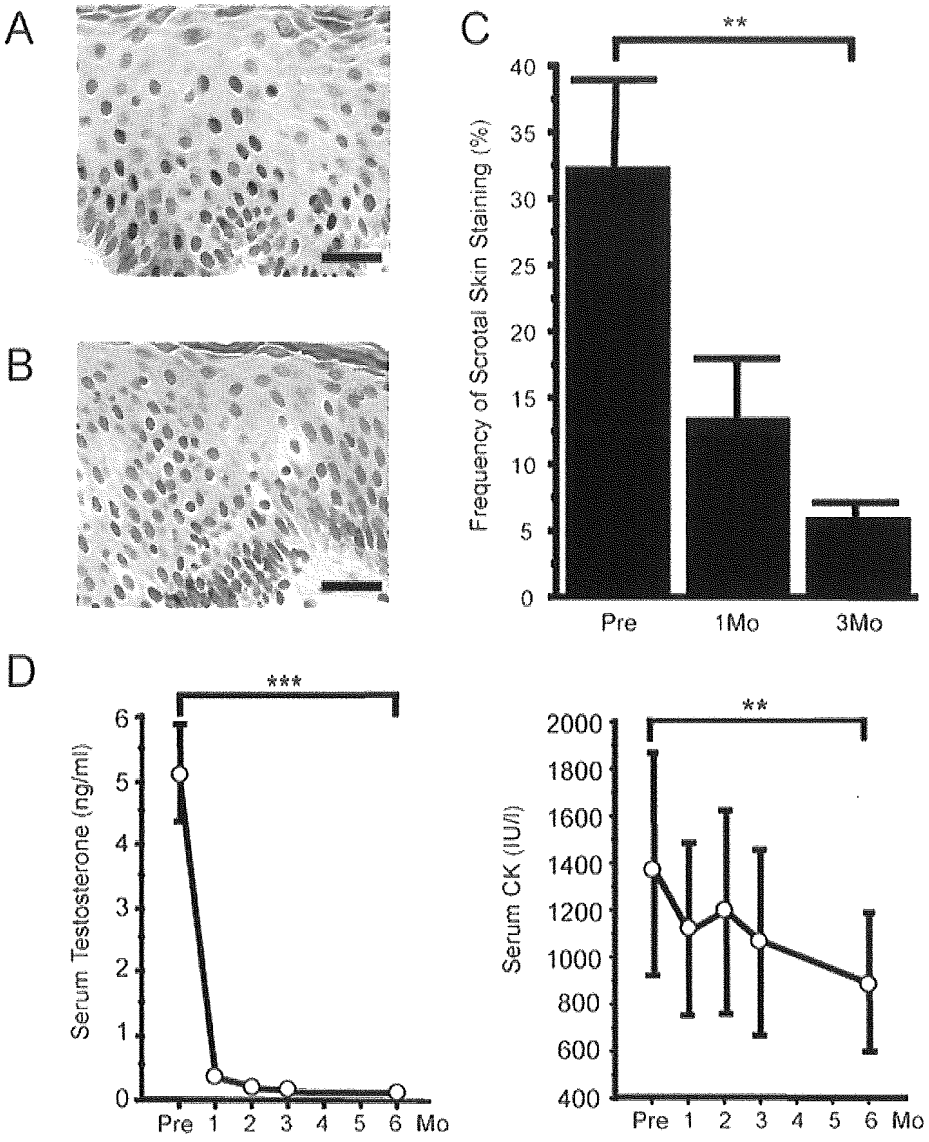

Fig 3. Effects of leuprorelin on mutant androgen receptor (AR) accumulation in scrotal skin, serum testosterone, and creatine kinase (CK). (A) Scrotal skin shows intense and frequent staining for anti-polyglutamine antibody in the nucleus before therapy. (B) Twelve weeks after therapy, both intensity and frequency of nuclear staining markedly decreased. Bar = 30μm. (C) Quantitative analysis of immunohistochemistry demonstrated a significant decrease in the number of positively stained nuclei. (D) Serum testosterone and CK decreased significantly in 6 months. Frequency of staining was calculated from counts of more than 500 nuclei in randomly selected areas and was expressed as mean ± standard deviation for 5 patients. $^{**}p < 0.01$; $^{***}p < 0.0001$.

Although our results were obtained from a small sample, nuclear accumulation of mutant AR in the scrotal skin appears to be a potent pathogenic biomarker of SBMA. A correlation between decline in validated clinical scales and nuclear mutant AR accumulations must be demonstrated in a longitudinal study to verify this histopathological feature as a biomarker for clinical severity. Similarly, validation of the scrotal skin biopsy findings as a surrogate end point in clinical trials will require a longitudinal study verifying that suppression of nuclear staining correlates with improvement on a validated clinical scale and the true clinical outcome events such as the need for a wheelchair, the presence of aspiration pneumonia, or death.

This work was supported by grants from the Ministry of Education, Culture, Sports, Science and Technology, Japan (17204032, G. S., M. D., F. T.); the Ministry of Health, Labor and Welfare, Japan (H-15-Kokoro-020, G. S., M. D.); and the Center for Clinical Trials, Japan Medical Association (G.S.).

We thank Dr N. Hishikawa for technical assistance.